



INŽENÝRSKÁ MECHANIKA 2005

NÁRODNÍ KONFERENCE

s mezinárodní účastí

Svratka, Česká republika, 9. - 12. května 2005

MESHLESS MODELLING OF URINE FLOW

L. Lobovský*, M. Horák*, J. Křen*

Summary: *The paper presents a mathematical model of urine flow inside a male urinary system. The problem is simulated as an isothermal transient flow of Newtonian fluid, which is modelled by smoothed particle hydrodynamics (SPH). The basic theory of SPH, which is a meshless method using a Lagrangian approach to fluid flow modelling, is presented. Results of SPH simulations are compared with results gained using other numerical methods.*

1. Introduction

The dynamics of urine flow through a male urinary system presents a complex problem featuring an interaction of fluid and deformable wall. The urine is emitted from a bladder through a urethra. The value of bladder pressure, which forces the urine out, depends on the phase of emission. That causes a transient flow of urine. The pressure of outflowing urine opens the cross-sectional profile of urethra, which is flattened in the relaxed state. During the emission, the urethra wall is stretched and the urethral flow becomes turbulent. The development of the urine flow along the urethral tube is influenced by a cross-sectional constriction of urethra at the part of a bladder neck and a prostate. The urine is a thin aqueous solution and the tissue of urinary organs is anisotropic non-linear viscoelastic material.

The presented study concerns mainly about a methodology of urine flow modelling. It presents a gridless approach to fluid flow simulations and its comparison with the grid-based calculations. Thus the problem of emission is significantly simplified. The study is focused on the urine flow in the phase of urination, when a urethral wall is fully stretched. The emission is modelled as a stationary isothermal flow of a Newtonian fluid through a channel with a cross-sectional constriction. The bladder shape is neglected and the channel wall is supposed to be rigid, i.e. the interaction of the fluid with the deformable wall is neglected as well. Body forces, e.g. gravity, and the outer atmospheric pressure are set to be zero. The main focus is taken on a development and an application of the Smoothed Particle Hydrodynamics code, which represents the gridless approach. The acquired results are compared with results of the simulations based on the Finite Element Method, belonging to the family of the grid-based methods.

* Ing. Libor Lobovský, Ing. Miroslav Horák, Ph.D., Prof. Ing. Jiří Křen, CSc.: Department of Mechanics, University of West Bohemia in Pilsen; Univerzitní 22; 30614 Plzeň; tel.: +420 377 632 330, fax: +420 377 632 302, e-mail: lobo@kme.zcu.cz

2. Method

Smoothed Particle Hydrodynamics (SPH) is a meshless Lagrangian numerical method originally introduced to solve gas dynamics problems in astrophysics. The continuum is discretised by a finite set of interpolating points called particles, which move according to the movement of the continuum and carry its physical characteristics. The SPH particles are not real material particles, but represent a finite volume, which has its center at the position of the particle. Every particle has assigned its invariant mass and variable physical characteristics (e.g. momentum, energy), which are determined by an interaction with neighbouring particles according to the modelled problem.

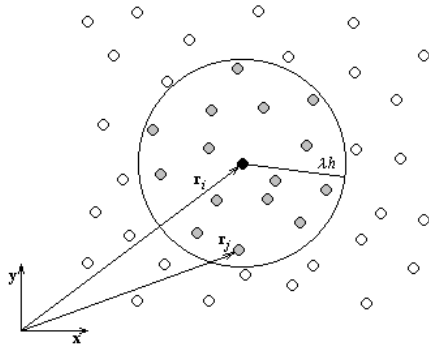


Fig.1 SPH particle interaction

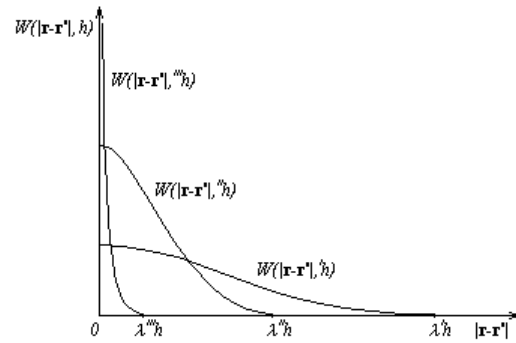


Fig.2 Smoothing function

The SPH formalism is based on the mathematical idea of the Dirac delta function and the interpolation theory. A continuous function f at a specific point \mathbf{r} of the continuous domain Ω is equal to an integral of the product of the function f at a specific point \mathbf{r}' and the Dirac delta function $\delta(\mathbf{r} - \mathbf{r}')$ over the entire domain

$$f(\mathbf{r}) = \int_{\Omega} f(\mathbf{r}') \delta(\mathbf{r} - \mathbf{r}') d\mathbf{r}'. \quad (1)$$

The Dirac delta function has the following properties:

$$\begin{aligned} \delta(\mathbf{r} - \mathbf{r}') &= 0, & \text{for } \mathbf{r}' \neq \mathbf{r}, \\ \int_{\Omega} \delta(\mathbf{r} - \mathbf{r}') d\mathbf{r}' &= 1. \end{aligned} \quad (2)$$

For numerical calculations, it is necessary to approximate the Dirac delta function with another analytical function W (fig. 2), which is continuous and fulfil the conditions

$$\begin{aligned} W(|\mathbf{r} - \mathbf{r}'|, h) &= 0, & \text{for } |\mathbf{r} - \mathbf{r}'| > \lambda h, \\ \int_{\Omega} W(|\mathbf{r} - \mathbf{r}'|, h) d\mathbf{r}' &= 1, \\ \lim_{h \rightarrow 0} W(|\mathbf{r} - \mathbf{r}'|, h) &= \delta(\mathbf{r} - \mathbf{r}'). \end{aligned} \quad (3)$$

The smoothing function W depends on two parameters, the distance between two points $|\mathbf{r} - \mathbf{r}'|$ and the smoothing length h . The multiple of the smoothing length λh defines a region, where the smoothing function is non-zero. As shown in Lobovský (2003), if the first derive of W is continuous and the smoothing function or the function f or both of them vanishes to zero at infinity, the equation (1) yields

$$\begin{aligned} f(\mathbf{r}) &= \int_{\Omega} f(\mathbf{r}') W(|\mathbf{r} - \mathbf{r}'|, h) d\mathbf{r}', \\ \nabla f(\mathbf{r}) &= - \int_{\Omega} f(\mathbf{r}') \nabla' W(|\mathbf{r} - \mathbf{r}'|, h) d\mathbf{r}', \end{aligned} \quad (4)$$

where ∇' denotes a derivative according to \mathbf{r}' .

The equations (4) can be discretised using a relationship between the volume represented by the particle and its mass and density

$$\int_{\Omega} d\mathbf{r}' = \sum_j \frac{m_j}{\rho_j}. \quad (5)$$

The particle mass m_j is fixed, while its density ρ_j may vary with the flow. In case the function f is evaluated at a particle i , its value is determined as a sum of contributions of all neighbouring particles (indexed with j)

$$\begin{aligned} f_i &= \sum_j \frac{m_j}{\rho_j} f_j W(|\mathbf{r}_i - \mathbf{r}_j|, h), \\ \nabla_i f_i &= \sum_j \frac{m_j}{\rho_j} f_j \nabla_i W(|\mathbf{r}_i - \mathbf{r}_j|, h). \end{aligned} \quad (6)$$

The second equation (6) is derived with respect to the relation (7) where ∇_i denotes a derivative according to i coordinates.

$$-\nabla_j W(|\mathbf{r}_i - \mathbf{r}_j|, h) = \nabla_i W(|\mathbf{r}_i - \mathbf{r}_j|, h). \quad (7)$$

In general, all SPH equations can be derived by the application of the equations (6) to governing equations describing an analysed problem. Within a fluid flow analysis, the set of governing equations consists of the continuity equation, the equation of motion, the energy equation and the equation of state.

$$\begin{aligned} \frac{d\rho}{dt} &= -\rho \nabla \cdot \mathbf{v}, \\ \frac{d\mathbf{v}}{dt} &= -\frac{1}{\rho} \nabla p, \\ \frac{du}{dt} &= -\frac{p}{\rho} \nabla \cdot \mathbf{v}, \\ p &= p(\rho). \end{aligned} \quad (8)$$

where ρ is the density, \mathbf{v} is the velocity vector, p is the pressure and u is the internal energy of the modelled fluid. Applying the relations (6) to set of equations (8) yields the SPH formulation of governing equations describing an isothermal flow of inviscid fluid.

$$\begin{aligned}
\frac{d\rho_i}{dt} &= \sum_j m_j (\mathbf{v}_i - \mathbf{v}_j) \cdot \nabla_i W_{ij}, \\
\frac{d\mathbf{v}_i}{dt} &= -\sum_j m_j \left(\frac{p_i}{\rho_i^2} + \frac{p_j}{\rho_j^2} \right) \nabla_i W_{ij}, \\
\frac{du_i}{dt} &= \frac{1}{2} \sum_j m_j \left(\frac{p_i}{\rho_i^2} + \frac{p_j}{\rho_j^2} \right) (\mathbf{v}_i - \mathbf{v}_j) \cdot \nabla_i W_{ij}, \\
p_i &= p_i(\rho_i).
\end{aligned} \tag{9}$$

The index i, j respectively, denotes variables at the particle i, j respectively, W_{ij} is a smoothing function $W(|\mathbf{r}_i - \mathbf{r}_j|, h)$.

The form of the state equation in (9) depends on a kind of fluid represented by particles. In case the simulated fluid is an ideal gas, the state equation becomes

$$p_i = (\kappa - 1) \rho_i u_i. \tag{10}$$

If the modelled fluid is supposed to be a slightly compressible liquid, the state equation may be defined as follows

$$p_i = {}^0 p_i + K \left[\left(\frac{\rho_i}{{}^0 \rho_i} \right)^\gamma - 1 \right], \quad \text{where } K = {}^0 \rho \frac{c^2}{\gamma}. \tag{11}$$

Upper left indices 0 denotes the initial variables at the beginning of the calculation. The bulk modulus K depends on a square of the sound speed, the initial density and the parameter γ which is usually taken as $\gamma = 7$. In case the modelled liquid is incompressible, the speed of sound is assumed to be higher or equal to ten times the maximum velocity in the entire fluid volume.

It is impossible to model a truly incompressible fluid with an SPH approximation. Discretisation of the governing equations is based on the relation (5), where the mass related to each particle is constant while its density can vary according to the behaviour of the given fluid. The pressure is an explicit function of the density, so the fluid flow is driven by local density fluctuations. Thus a quasi-incompressible approximation of incompressible fluid, such as equation (11), is necessary.

The SPH governing equations (9) do not contain any dissipative term. That disables modelling of viscous flows and it could be a reason of numerical instabilities. When shocks occur during the simulation, the absence of dissipative terms may cause a creation of large unphysical oscillations. In order to stabilise the calculation and to smooth the shock oscillations, the artificial viscosity is introduced. It helps to prevent particle interpenetration and particle trajectory crossing. It is defined as a form of viscous pressure and included within the pressure term in governing equations

$$\begin{aligned}\frac{d\mathbf{v}_i}{dt} &= -\sum_j m_j \left(\frac{p_i}{\rho_i^2} + \frac{p_j}{\rho_j^2} + \Pi_{ij} \right) \nabla_i W_{ij}, \\ \frac{du_i}{dt} &= \frac{1}{2} \sum_j m_j \left(\frac{p_i}{\rho_i^2} + \frac{p_j}{\rho_j^2} + \Pi_{ij} \right) (\mathbf{v}_i - \mathbf{v}_j) \cdot \nabla_i W_{ij}.\end{aligned}\quad (12)$$

The artificial viscosity Π_{ij} is usually defined as a combination of terms analogous to bulk and von Neumann-Richtmeyer viscous pressures used in finite difference methods.

$$\begin{aligned}\Pi_{ij} &= \frac{2}{\rho_i + \rho_j} \left(-\alpha \frac{c_i + c_j}{2} \mu_{ij} + \beta \mu_{ij}^2 \right), \\ \mu_{ij} &= \begin{cases} \frac{1}{2} (h_i + h_j) \frac{(\mathbf{v}_i - \mathbf{v}_j) \cdot (\mathbf{r}_i - \mathbf{r}_j)}{|\mathbf{r}_i - \mathbf{r}_j|^2 + \eta^2}, & (\mathbf{v}_i - \mathbf{v}_j) \cdot (\mathbf{r}_i - \mathbf{r}_j) < 0, \\ 0, & (\mathbf{v}_i - \mathbf{v}_j) \cdot (\mathbf{r}_i - \mathbf{r}_j) \geq 0, \end{cases}\end{aligned}\quad (13)$$

where c_i is a speed of sound, h_i is a smoothing length, α and β are constant artificial viscosity parameters and η is an anti-crossing parameter $\eta^2 = 0.01h^2$, where h is an average smoothing length $h = (h_i + h_j)/2$. The term Π_{ij} is positive when particles are moving together and null otherwise.

The denotation of the artificial viscosity is a bit controversial, as it does not have a dimension of viscosity. Although the artificial viscosity introduces dissipative effects permitting the viscous flow modelling, there is no analytical prove of its ability to substitute the physical viscosity, which is represented by a dissipation term in the Navier-Stokes equation of motion

$$\frac{d\mathbf{v}}{dt} = -\frac{1}{\rho} \nabla p + \nu \nabla^2 \mathbf{v} + \frac{1}{\rho} \mathbf{F}. \quad (14)$$

The dissipation term in (14) is defined as a multiplication of the kinematic viscosity ν and the second-order derivative of the velocity vector. Its SPH representation can be implemented using nested sums over the particles or using the second-order differentiation of the smoothing function. But the first approach produces very high computational effort and the second one may significantly decrease the calculation accuracy. An alternative SPH approximation of the viscous term can be derived as

$$\left[\left(\frac{1}{\rho} \nabla \cdot \mu \nabla \right) \mathbf{v} \right]_i \approx \sum_j \frac{m_j}{\rho_i \rho_j} \frac{\mu_i + \mu_j}{|\mathbf{r}_i - \mathbf{r}_j|^2 + \eta^2} [(\mathbf{r}_i - \mathbf{r}_j) \cdot \nabla_i W_{ij}] (\mathbf{v}_i - \mathbf{v}_j), \quad (15)$$

where μ is the dynamic viscosity $\mu = \rho\nu$ and the resulting equation of motion becomes

$$\frac{d\mathbf{v}_i}{dt} = -\sum_j m_j \left(\frac{p_i}{\rho_i^2} + \frac{p_j}{\rho_j^2} \right) \nabla_i W_{ij} + \sum_j \frac{m_j}{\rho_i \rho_j} \frac{\mu_i + \mu_j}{|\mathbf{r}_i - \mathbf{r}_j|^2 + \eta^2} [(\mathbf{r}_i - \mathbf{r}_j) \cdot \nabla_i W_{ij}] (\mathbf{v}_i - \mathbf{v}_j) + \frac{\mathbf{F}_i}{\rho_i}. \quad (16)$$

During high-speed flow or free surface simulations, an unphysical particle motion may occur. In such case the correction of particle motion may be applied. It is a stabilising term taking an average velocity of all neighbouring particles into account.

$$\frac{d\mathbf{r}_i}{dt} = \mathbf{v}_i + \varepsilon \sum_j m_j \frac{\mathbf{v}_i - \mathbf{v}_j}{\frac{1}{2}(\rho_i + \rho_j)} W_{ij}. \quad (17)$$

A constant parameter ε is from an interval $\langle 0, 1 \rangle$. The second term on the right hand side of the equation (17) helps to keep particles ordered and helps to prevent a penetration of one fluid by another.

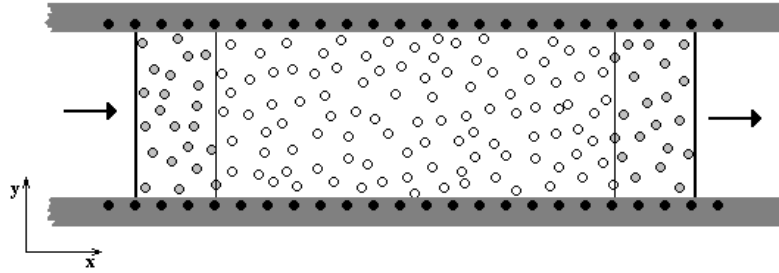


Fig.3 Modelling of boundary conditions

Boundaries of a fluid represented by smoothed particles can be modelled by other particles (fig. 3). The simplest way of boundary modelling uses the boundary particles that line the interface between the fluid and the wall. Their properties are determined according to the character of the current interface. The interaction between boundary and fluid particles can be defined as a force similar to the Lennard-Jones force between molecules.

$$f = \begin{cases} D \frac{\mathbf{r} - \mathbf{r}_B}{|\mathbf{r} - \mathbf{r}_B|^2} \left[\left(\frac{r_{B0}}{|\mathbf{r} - \mathbf{r}_B|} \right)^{p_1} - \left(\frac{r_{B0}}{|\mathbf{r} - \mathbf{r}_B|} \right)^{p_2} \right], & |\mathbf{r} - \mathbf{r}_B| < r_{B0}, \\ 0, & |\mathbf{r} - \mathbf{r}_B| \geq r_{B0}. \end{cases} \quad (18)$$

The force $f = f(|\mathbf{r} - \mathbf{r}_B|)$ is a function of the distance between the boundary and the fluid particle, where \mathbf{r} denotes the fluid particle position and \mathbf{r}_B states the position of the boundary particle. The length scale r_{B0} , which determines the distance of the boundary force influence, is usually taken to be an initial spacing between fluid and boundary particles. Parameters D , p_1 and p_2 are constants chosen regarding to the physical configuration of the simulation in order to get a force function, which is strongly peaked for the fluid particles getting too close to the boundary.

When the no-slip boundary conditions are prescribed, it is necessary to include an influence of the boundary particles in the sum of viscous terms in the equation of motion for the fluid particles within a thin layer along the boundary. The satisfactory width of such layer can be taken as a half of the smoothing function support λh . Then, the effect of the boundary particle j on the fluid particle i is described as

$$\sum_{j \in \mathcal{B}} (m_j \Pi_{ij} \nabla_i W_{ij} + f_{ij}), \quad (19)$$

where \mathcal{B} is a set of all interacting boundary particles.

The flow of the modelled fluid is defined by external forces and by initial and boundary conditions. The SPH flow boundary conditions (fig. 3) define regions in space where the fluid particles get into the influence of the pressure or velocity boundary conditions. The sphere of the boundary influence is defined by the smoothing function support λh . In case the fluid particle passes out of the computational domain through the flow boundary, it is removed from the calculation and set to be inactive, i.e. it is discarded from the calculation. In case there is an inflow boundary defined, new particles representing the fluid can be activated and inserted at the inflow when the fluid particles move inwards the computational domain. If the SPH simulation is implemented for a constant number of particles and inflow boundary is applied, an appropriate amount of inactive particles should be stored. Application of SPH flow boundary conditions enables creation of arbitrary transient flows as well as arbitrary velocity profiles at the boundaries.

3. Examples and Discussion

The SPH code was tested on elementary examples of urethral flow and its results were compared to results of computations performed by the Finite Element Method (FEM) code developed in (Křen et al., 2001).

Two simple examples are presented. Both of them are solved as an isothermal flow of quasi-incompressible (SPH) and incompressible (FEM) fluid. During the SPH simulations, the urethra wall is modelled as a single layer of static boundary particles and the inflow and the outflow boundary conditions are applied. At the beginning of every SPH calculation, the urine is represented by a regular initial distribution of fluid particles throughout the computational domain.

First, the capability of modelling the viscous fluid is tested on a flow through a straight channel (stretched urethra). The urine flow is driven by a pressure gradient. The hydrostatic pressure is taken as zero. The normed relative pressure is set to one at the inflow and to zero at the outflow. An anti-penetration and no-slip boundary conditions are implemented. The length scale of a boundary influence is assumed to be equal to the distance between particles during their initial distribution for the anti-penetration condition and twice as much for the no-slip boundary condition. In the fluid state equation (11), the value of sound speed is set to one hundred meters per second and the parameter γ was equal 7. The artificial viscosity is applied. The value of both artificial viscosity parameters α and β is 2. The anti-crossing parameter η is used as defined above, i.e. it is equal to one tenth of the smoothing length. Other urine characteristic, such as the density and the dynamic viscosity, are considered comparable to properties of water. The urine density is equal to thousand kilograms per cubic meter and the dynamic viscosity is set to 0.001 kilograms per meter and second.

Figures 4 and 5 show the distribution of the normed velocity in the straight urethral channel. Results of the SPH simulation (fig. 4) showed that the no-slip boundary condition and the dissipative terms included within the equations of motion are capable of modelling the viscous character of the flow, eventhough the velocity profile through the channel cross-section acquired from the SPH simulation is flattened in comparison to the result of FEM calculation (fig. 5).

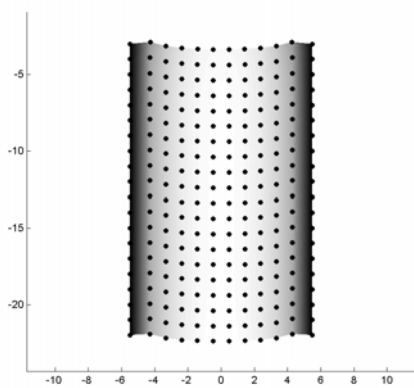


Fig.4 SPH flow through a straight urethra:
velocity distribution

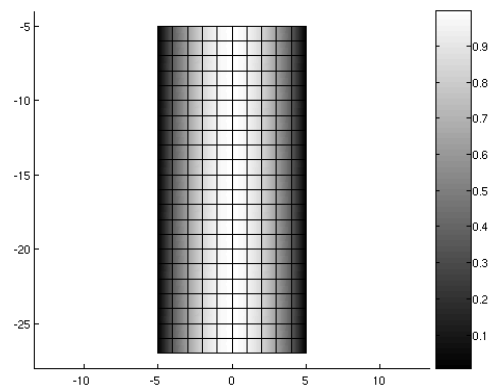


Fig.5 FEM flow through a straight urethra:
velocity distribution

The second example presents the flow through a narrowed channel. The narrowing of the channel represents the urethra necking at the prostate region. The urine parameters are kept the same as in the previous example. Its flow is driven by pressure boundary conditions. The normed inflow pressure is taken as one and the outflow pressure is kept zero. The hydrostatic pressure is neglected. The distance of the anti-penetration boundary condition influence is equal to the initial spacing between particles, while the influence of the no-slip boundary condition is equal to its 1.6 multiple.

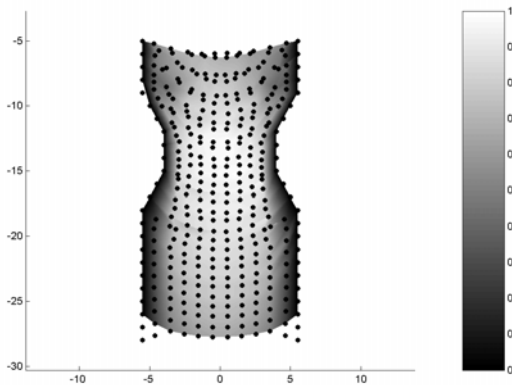


Fig.6 SPH flow through narrowed urethra:
velocity distribution

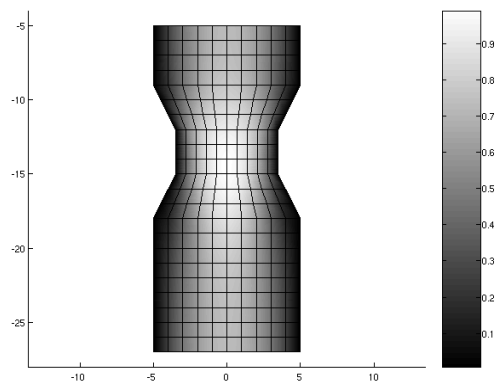


Fig.7 FEM flow through narrowed urethra:
velocity distribution

The results of both SPH and FEM computations (figures 6-7) show a similar character of the development of the urine flow through the narrowed channel. The resulting distribution of the normed velocity field is comparable in both calculations.

The development of a velocity profile within the SPH simulations is influenced by the fact that the modelled fluid is not trully incompressible. Slight changes in the fluid volume may be observed. Very important factor influencing the calculation accuracy is an appropriate definition of the boundary condition. The reliability of SPH simulations may be also

influenced by its initial configuration determining the number and the spatial distribution of neighbouring particles. In case the ordering effects may occur, an irregular particle distribution should be applied.

The SPH simulations require significantly longer CPU time than FEM computations. The main factors influencing the computational efforts are the total number of particles and the range of the smoothing function determining the number of interacting neighbouring particles. During the modelling of complex fluid flows, a higher number of particles may be required in order to model the problem accurately. The advantage of SPH method is the absence of a computational grid and its applicability to a wide range of problems.

4. Acknowledgement

This work is supported by the Grant Agency of the Czech Republic (GA ČR) as a part of the grant no. 106/04/0201.

5. References

- Křen, J., Horák, M., Zátura, F., Rosenberg, M. (2001) Mathematical Model of the Male Urinary Tract. *Biomedical Papers*, 145, 2, pp.91-96.
- Lobovský, L. (2003) *Application of SPH in Fluid Mechanics*. Diploma Thesis, ZČU, Plzeň.